Characterization of anodic spark-converted titanium surfaces for biomedical applications

J. P. SCHRECKENBACH, G. MARX
Department of Chemistry, Technical University of Chemnitz, D-09107 Chemnitz, Germany
F. SCHLOTTIG, M. TEXTOR, N. D. SPENCER
ETH Zürich, Laboratory for Surface Science and Technology, Department of Materials, CH-8092 Zürich, Switzerland

The aim of the present study was to characterize the surface morphology, microstructure and the chemical composition of anodic spark-converted titanium surfaces. The coatings were prepared in an electrochemical cell by the anodic spark deposition technique in an aqueous solution of $Ca(H_2PO_4)_2$. The coatings were characterized by X-ray photoelectron spectroscopy (XPS), scanning electron microscopy (SEM), electron probe microanalysis (EPMA) and X-ray diffraction (XRD). The properties of the coatings are described in terms of morphology.

1. Introduction

Titanium and titanium alloys are increasingly being used as implant materials as a result of the very good bulk properties of titanium (alloys) and the excellent biocompatibility of its surface oxides [1]. In this way the mechanical properties of the metal are combined with the advantageous surface chemical properties of the oxide. Based on the negative electrode potential of titanium relative to the standard hydrogen electrode (SHE), titanium ought to react in aqueous media by evolving hydrogen. But, just as in the case of aluminum, a dense adherent passivating oxide film protects the highly active underlying metal.

This natural titanium oxide film that grows spontaneously at room temperature has a thickness of about 5 nm [2]. Damaged films become immediately repassivated in the presence of oxygen and/or water. At the metal/oxide interface the substoichiometric titanium oxides TiO_{2-x} are present, while at the outermost surface, the composition approximately corresponds to the stoichiometry of a TiO_2 phase [3]. An additional hydration of the oxide surface may be important in establishing a suitable environment for biomolecules. Because of the dominating influence of the titanium surface oxides on the biocompatibility of the titanium implants, extensive efforts have been undertaken to improve our understanding of the complex processes occuring at the metal/oxide/tissue boundaries [4, 5].

Many investigations have been carried out with the aim of developing and applying novel surface coating techniques to improve wear resistance, chemical stability and biocompatibility of the titanium surface. For example, coatings consisting of microscopic glass-ceramic powder particles flame or plasma sprayed onto the surfaces of metal implants, mostly titanium alloys, have shown success in clinical applications [6]. Fast bone ingrowth and bridging to the implant have been reported for plasma sprayed hydroxyapatite and fluoroapatite coatings [7]. Sol–gel derived titania coatings, formation of nanophase hydroxyapatite on cathodically polarized electrodes and anodic electrophoretic deposition of hydroxyapatite have all been investigated [8–10].

Anodic spark deposition (ASD) is an advanced coating process for producing inorganic glass-ceramic-like coating structures on to valve metal surfaces with adhesive strength up to 25 MPa [11–14]. ASD takes place during the dielectric breakdown of an insulating oxide film at the surface of a metal anode in contact with a suitable electrolyte and is accompanied by visible plasma-like micro sparking at the anode surface. The resulting conversion coating is composed of compounds containing elements from both the anode metal and the electrolyte constituents.

The present study was undertaken to produce and characterize the surface morphology, the microstructure and the chemical composition of anodic-spark-converted titanium surfaces for medical applications.

2. Material and methods

2.1. ASD coating procedure

The coatings were prepared in an electrochemical cell by the anodic spark deposition technique, using a computer controlled d.c. Heinzinger PHN power supply. Aqueous solutions of $0.12\,mol\,l^{-1}$ AR grade $Ca(H_2PO_4)_2$ and $0.8\,mol\,l^{-1}$ AR grade NaF and Na_2CO_3 were used as electrolytes. A titanium foil (Aldrich) of $10 \times 10\,mm^2$, 0.127 mm thickness and 99.7% purity was used as the anode and platinum wire as cathode.

The titanium samples were chemically polished for 10 s in a mixture of hydrofluoric and nitric acid (HF/HNO_3) in a 1 : 1 ratio and ultrasonically cleaned in water followed by acetone rinsing. First, a pre-spark film was potentiodynamically formed with $30\,mA\,cm^{-2}$ until sparking occurred at a potential of 165 V. The ASD current density was up to $1\,A\,cm^{-2}$. After the coating

process, the specimens were rinsed in distilled water, dried and stored in an argon atmosphere.

2.2. Surface characterization

X-ray photoelectron spectra (XPS) were recorded on a SAGE 100 (SPECS, Berlin) using non-monochromatized MgK_{α} radiation at 300 W (12 kV, 25 mA) and an electron detector pass energy of 50 eV for survey and 14 eV for high-resolution scans resulting in a full width half maximum (FWHM) of silver Ag 3d5/2 of 1 eV. The residual pressure during analysis was always below 5×10^{-8} Pa. The samples were mounted as coated titanium foils. Because of a shift due to charging of the sample, the C1s spectrum–resulting from surface contaminated hydrocarbons–was used as reference peak at 285.0 eV.

X-ray diffractograms were taken using a Siemens D-5000 diffractometer. The scanning electron microscopy (SEM) investigations were performed on a Jeol JSM 840 A and the electron probe microanalysis (EPMA) was carried out on a Cameca SX100.

3. Results and discussion

3.1. Morphology and composition

In contrast to thermally generated or pre-spark-region-generated titanium oxide films, the conversion coatings fabricated by ASD show a micron-sized morphology and topography. Due to the plasma-like state of the surface during ASD and the resulting oxide fusion, the anodically erupted gases oxygen and steam can form a characteristic surface morphology of clearly visible melted oxide and a spongy interconnected microstructure (Fig. 1).

The size of the morphological surfaces features and the pore diameters are in the range of 1–5 μm, the film thickness is up to 10 μm. The surface morphologies can be modified through variation of the electrical parameters and the electrolyte composition. Fig. 2 shows a sample that was generated in an electrolyte containing Na_2CO_3. The technique therefore has the potential to produce surface morphology and porosity specifically designed to favor a particular response of the tissue. Also, the defined pore size structure may be of value as a depot for bioactive constituents such as growth factors or bone morphogenic proteins.

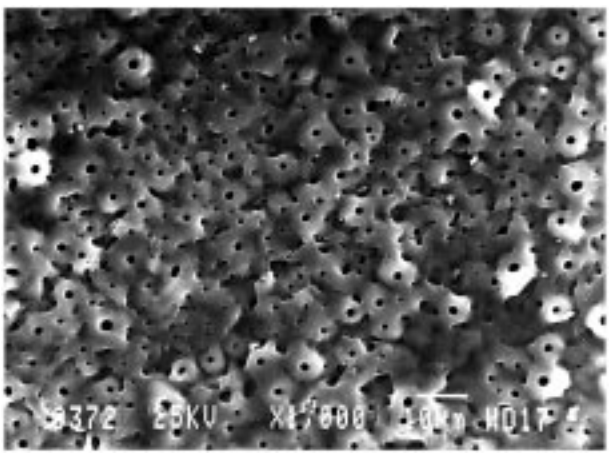

Figure 1 Scanning electron micrograph of the microstructured ASD surface ($Ca(H_2PO_4)_2$ electrolyte).

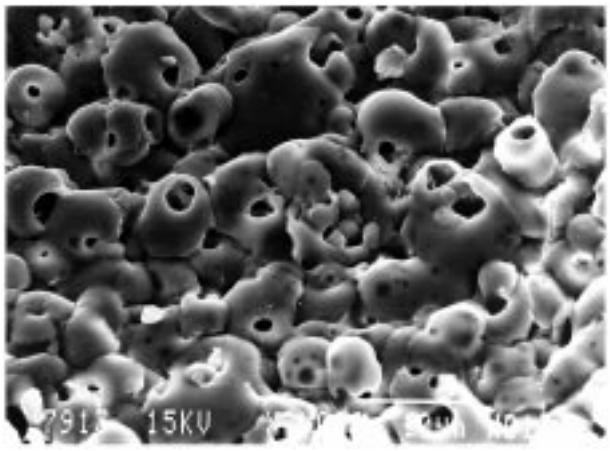

Figure 2 Scanning electron micrograph of the microstructured ASD coating (Na_2CO_3 containing electrolyte).

For the described experimental conditions, X-ray diffraction of the conversion coatings exhibit only diffraction patterns that can be attributed to the 0 0 2, 1 0 1 and 1 0 2 planes of the hexagonal titanium metal system.

Neither the titanium oxide phases anatase or rutile nor Ca/P compounds could be found through X-ray diffraction, which points to the glassy amorphous nature of the coatings. Investigations of the chemical composition of the coatings by means of electron probe microanalysis, reveal a high concentration of Ca and P relative to titanium (Fig. 3). The average ratio of the atomic concentrations of Ca : P are close to 1 : 2.

High-resolution X-ray photoelectron spectra were acquired for C1s, O1s, P2p, Ca2s and Ti2p. These core level binding energy peaks have been used to characterize the chemical state of these elements at the surface region of the coating. The broad O1s peak (FWHM = 2.4 eV) indicates the presence of different oxygen-containing species at the outermost surface. The predominant O (1 s) binding energy is 530.1 eV. A small shoulder at higher binding energies (531.9 eV) was also detected (Fig. 4).

The lower O1 s component may be assigned to Ca–O and Ti–O species in agreement with published data [5]. The shoulder at higher binding energy is attributed to P–O and O–H groups, known to have typical values between 531 and 533 eV [15]. The P2p spectra indicate

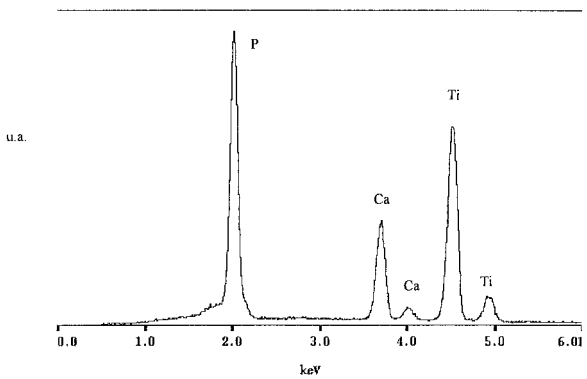

Figure 3 EPMA of the X-ray amorphous ASD coating showing the presence of P and Ca.

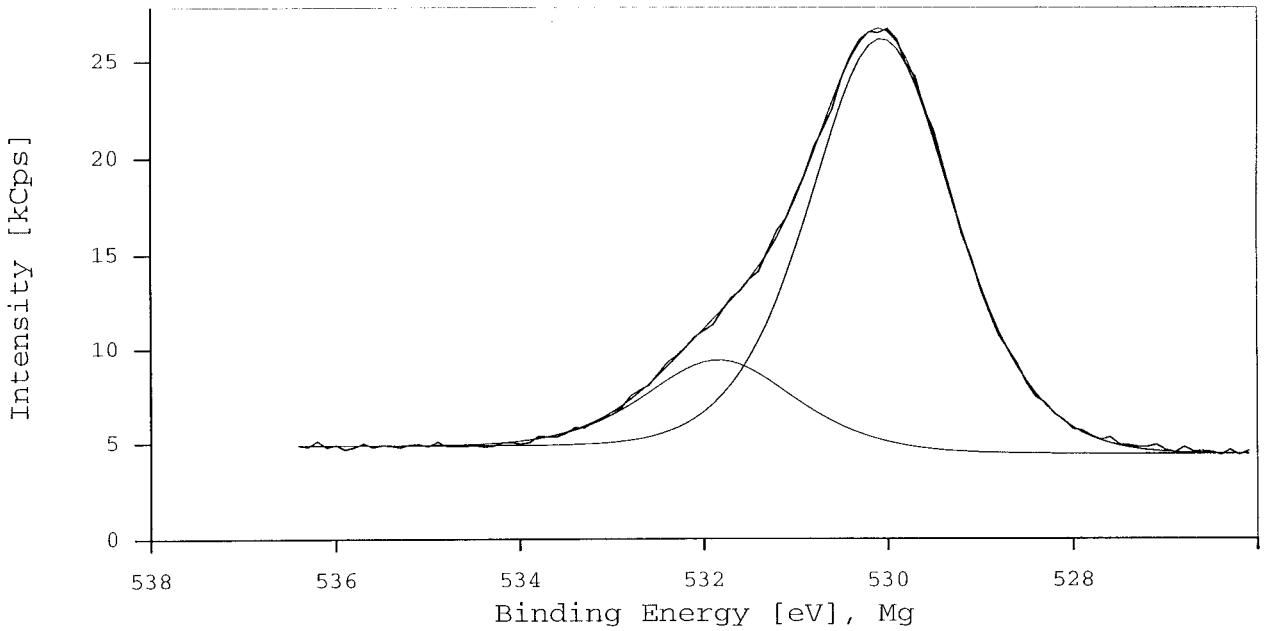

Figure 4 XPS O1s high resolution spectrum of the anodic-spark-deposited conversion coating ($Ca(H_2PO_4)_2$ electrolyte).

the presence of several P-containing species (maximum at 133.8 eV, FWHM = 2.1 eV). The P (2p) curves were fitted taking into account the asymmetry of the P 2p signal due to the spin-orbit splitting ($2p_{3/2}, 2p_{1/2}$) of the single peaks. The conclusion is that the phosphorus is present at least in two different chemical states corresponding to XPS binding energies of 133.3 eV and 134.2 eV (Fig. 5).

The generation of different phosphates during the plasma-chemical ASD process is thermodynamically possible because the degree of the phosphate condensation increases with increasing temperature. On the basis of published data [16–18] we suggest the simultaneous presence of isolated $[PO_4]$ tetrahedra (133.5 eV) [19], pyrophosphate groups (134.4 eV) [19, 20] and polyphosphates. On the other hand the presence of amorphous compounds, for instance $Ca(H_2PO_4)_2 \cdot H_2O$, $Ti_3(PO_4)_4 \cdot nH_2O$ and $Ca_{10}(PO_4)_6(OH)_2$ may also contribute to the different P peaks [21].

The XPS Ti2p spectra (Fig. 6) show the expected doublet with $Ti2p_{3/2}$ at 459.2 eV and $Ti2p_{1/2}$ at 465.1 eV [2]. These peak positions are characteristic for Ti^{4+}, the highest oxidation state of titanium, present in TiO_2 and titanates. A minor intensity contribution to the $Ti2p_{3/2}$ peak is present in the region of titanium sub-oxides. This indicates that the coating also contains minor fractions of TiO_{2-x}. Recent electron-spin resonance investigations confirmed the existence of the paramagnetic Ti^{3+} species in ASD films on titanium. The Ca2p spectra reveal the expected doublet with $Ca2p_{3/2}$ at 347.6.5 eV and $Ca2p_{1/2}$ at 351.1 eV, typical for the Ca^{2+} oxidation state in inorganic calcium–oxygen compounds.

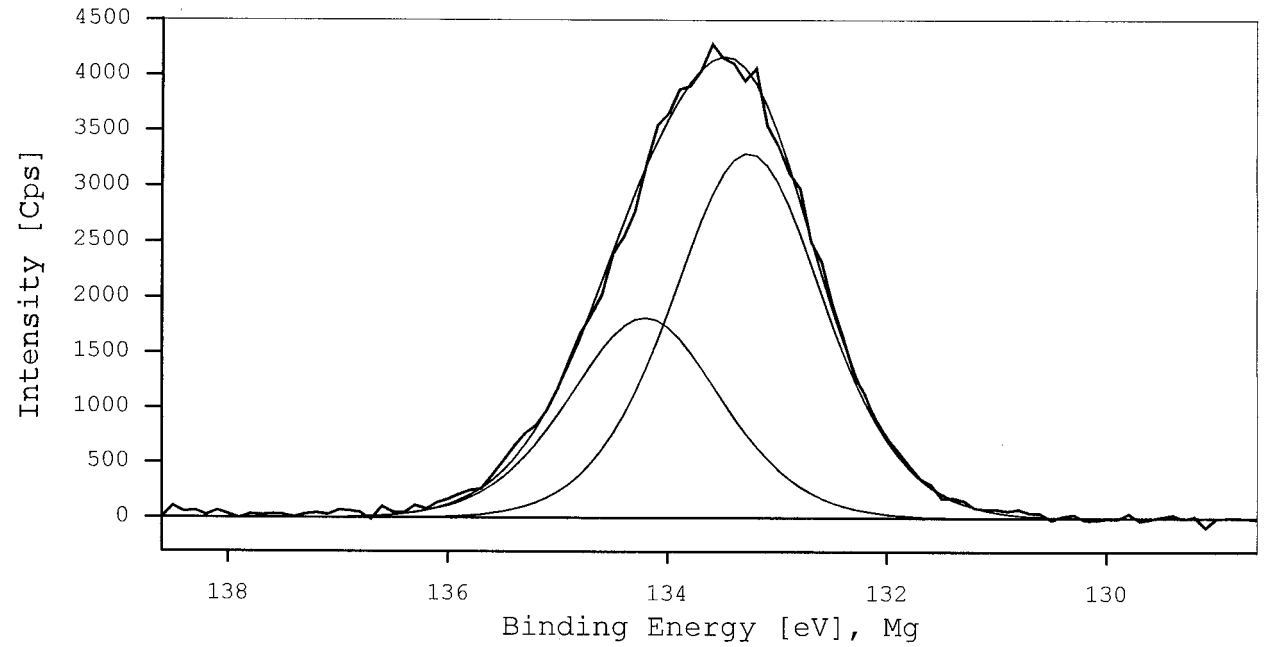

Figure 5 XPS P2p high resolution spectrum of the anodic-spark-deposited conversion coating ($Ca(H_2PO_4)_2$ electrolyte).

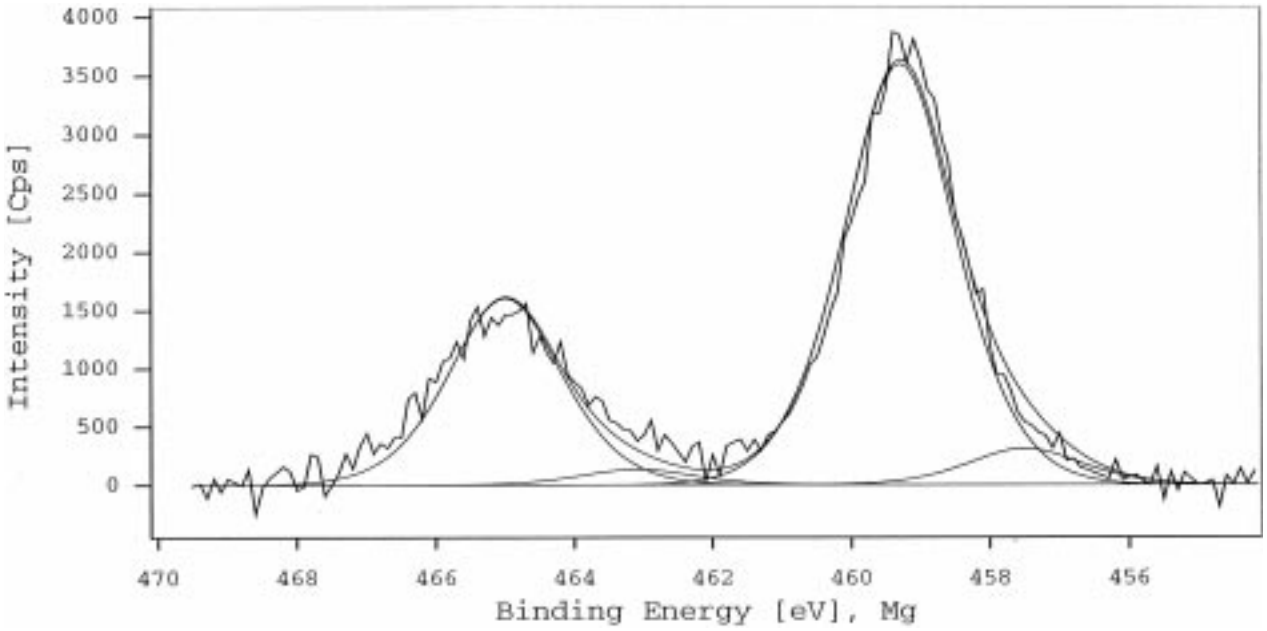

Figure 6 XPS Ti2p high resolution spectrum of the anodic-spark-deposited conversion coating ($Ca(H_2PO_4)_2$ electrolyte).

3.2. Structure of the coating

The results of the surface- and solid-state analytical investigations show that an X-ray amorphous glassy coating on the titanium has been formed under the described experimental conditions. The coatings are porous in the outermost surface region, with pore diameters of 1–5 μm. At the metal/oxide boundary a barrier film up to 1 μm in thickness is responsible for the high corrosion resistance of the ASD conversion coating (Fig. 7).

In agreement with the observed chemical composition and the ratio of Ti, O and P in the ASD coating, the structure can be described as a system of glassy solidified oxides. TiO_6 octahedra and PO_4 tetrahedra are believed to act as a network former by sharing corners or edges [22]. Because of their higher ion radius of 99 pm, calcium ions act as a modifier in the ternary glass matrix. Within the coating, the generation of nanocrystalline aggregations and cluster formations of the system $x\mathrm{CaO}/y\mathrm{P_2O_5}/z\mathrm{TiO_2}$ is likely (Fig. 8). Its identification is the subject of continuing investigations.

4. Conclusions

During anodic polarization of the titanium surface in a $Ca(H_2PO_4)_2$ electrolyte system, a titanium oxide barrier layer is formed first. Dielectric breakdown during the anodic spark deposition at higher voltages leads to increased film growth and a modification of this anodic film. A porous microstructured conversion coating results through the reaction between the titanium substrate and calcium and phosphate present in the aqueous electrolyte.

The formation of the glassy microstructured surface can be explained by the plasma-chemical and thermal reactions taking place during the ASD process.

The plasma-like state at the surface results in the fusion of the anodically formed oxides. Anodically

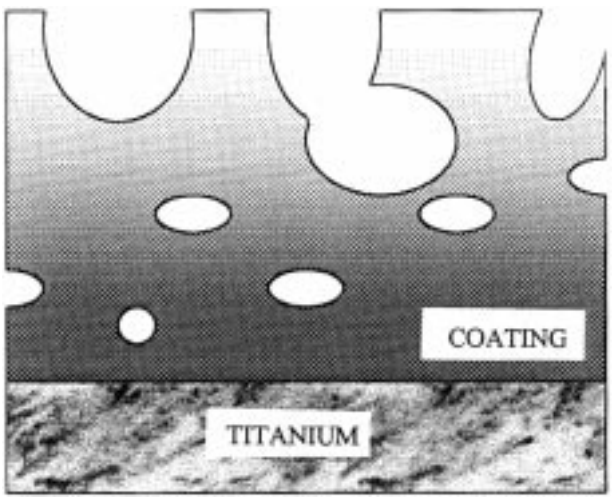

Figure 7 Schematic model of the pore distribution of an anodic-spark-deposited coating.

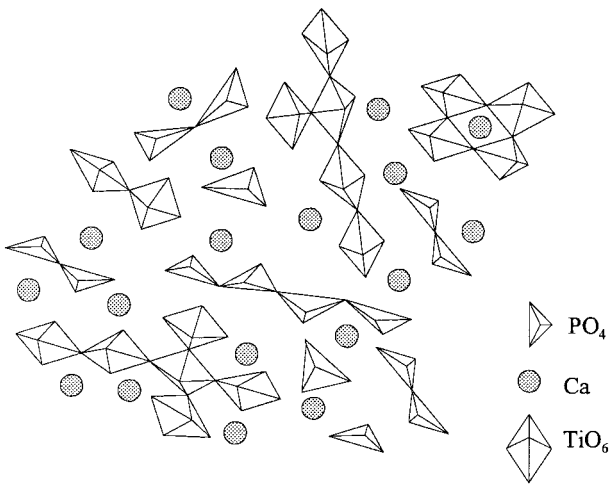

Figure 8 Schematic view of an ASD coating with an amorphous $CaO/P_2O_5/TiO_2$ structure.

produced gases, particularly oxygen and steam, are most likely the cause of the observed porosity of the oxide film. The glass-like composition contains network-forming PO_4 tetrahedras and TiO_6 octahedras in different degrees of condensation. Ca acts as an interstitial modifier oxide.

ASD coatings on titanium produced in calcium phosphate electrolytes are of potential interest for bone implants in view of their high abrasion resistance, excellent corrosion resistance and biocompatible composition. Future investigations will concentrate on improving and controlling the surface morphology and carrying out *in vitro* studies to determine the properties of these coatings for medical implant applications, as well as determining the chemical stability/dissolution rate of the calcium phosphate species in the coating.

Acknowledgments

The support of this work by the Swiss KTI Medtech initiative and by the Dr Robert Mathys Foundation, Bettlach, Switzerland is gratefully acknowledged.

References

1. D. S. SUTHERLAND, P. D. FORSHAW, G. C. ALLEN, I. T. BROWN and K. R. WILLIAMS, *Biomaterials* **12** (1993) 893.
2. C. SITTIG, M. TEXTOR, N. D. SPENCER, M. WEILAND and P. H. VALLOTTON, *J. Mater. Sci.: Mater. Med.* **10** (1999) 35.
3. P. TENGVALL and I. LUNDSTRÖM, *Clin. Mater.* **9** (1992) 115.
4. M. ASK, J. LAUSMAA and B. KASEMO, *Appl. Surf. Sci.* **35** (1989) 238.
5. E. LEITAO, M. A. BARBOSA and K. DE GROOT, *J. Mater. Sci.: Mater. Med.* **8** (1997) 423.
6. G. HEIMKE, *Adv. Mater.* **6** (1991) 320.
7. W. DHERT, *ESB News* **1** (1992) 4.
8. D. B. HADDOW, P. F. JAMES and R. VAN NOORT, *J. Mater. Sci.: Mater. Med.* **7** (1996) 255.
9. M. SHIKHANZADEH, *ibid.* **9** (1998) 67.
10. I. ZHITOMIRSKY and L. GAL-OR, *ibid.* **8** (1997) 213.
11. G. P. WIRTZ, S. D. BROWN and W. M. KRIVEN, *Mater. Manuf. Proc.* **6** (1991) 87.
12. US Patent No. 4846837 (1989).
13. J. SCHRECKENBACH and K. RABENDING, *J. Chem. Edu.* **8** (1996) 782.
14. F. SCHLOTTIG, J. SCHRECKENBACH and G. MARX, *Fresenius J. Anal. Chem.* **363** (1999) 209.
15. T. HANAWA and M. OTA, *Biomaterials* **12** (1991) 767.
16. G. N. RAIKAR, J. L. ONG and L. C. LUCAS, *Surf. Sci. Spectra* **4** (1997) 9.
17. E. HOROWITZ and J. E. PARR in ''Characterization and performance of calcium phosphate coatings for implants'' (ASTM Publication No. 04-011960-54, American Society for Testing and Materials, Philadelphia, 1994).
18. E. FLUCK and D. WEBER, *Pure Appl. Chem.* **44** (1975) 37.
19. W. E. MORGAN, J. R. VAN WAZER and W. J. STEC, *J. Amer. Chem. Soc.* **95** (1973) 751.
20. D. T. CLARK, T. FOK, G. G. ROBERTS and R. W. SYKES, *Thin Solid Films* **70** (1980) 261.
21. T. HANAWA in ''The bone–biomaterials interface'' (University of Toronto Press, Toronto, 1991).
22. W. VOGEL in ''Chemistry of Glass'' (Springer, Berlin, 1992).

Received 21 September
and accepted 21 September 1998